

The Minnesota inverted-tee system: Parametric studies for preliminary design

Roberto Piccinin and Arturo E. Schultz

- The Center City Bridge (MN bridge 13004), built in Minnesota using the Poutre-Dalle system developed in France, has been monitored for transverse load distribution and continuity over the pier since the deck was cast in September 2005.
- A two-span specimen was constructed in the laboratory to investigate the effects of variations in flange thickness, bursting reinforcement, horizontal shear reinforcement, and flange surface treatment to provide data for optimizing section design.
- Linear elastic finite element analyses were conducted to simulate the behavior of the system and were calibrated using results obtained from static tests of MN bridge 13004 and the laboratory specimen.
- For all of the cases investigated, the service stresses were found to control the design.

The precast concrete inverted-tee system (known in Europe as the Poutre-Dalle system) was adopted for use in Minnesota as an alternative to conventional systems for rapid replacement of bridges (Fig. 1). The system consists of a series of shallow precast concrete inverted-tee beams connected through transverse looped bars and a cast-in-place concrete slab to create continuity between the precast concrete members. The panels are joined longitudinally and are typically not held by post-tensioning nor overlaid at the top of the cast-in-place concrete slab. Advantages of cast-in-place concrete slabs in the field include ease of construction, enhanced structural continuity between members, and the ability to adjust the surface according to different needs.

Cast-in-place concrete slabs, however, require more-stringent quality control and have the tendency to crack due to restraint of volume changes caused by drying and thermal effects. The presence of reflecting cracks is of particular concern in states with cold-weather climates, such as Minnesota, where deicing chemicals can penetrate into cracks and corrode the reinforcement. In addition to corrosion, significant reflective cracking could lead to separation of the panels, resulting, for example, in a decrease in transverse load distribution.

Post-tensioning is usually used to join precast concrete members and is often considered necessary for the use

of precast concrete members in bridge superstructures. In fact, the compression provided by the post-tensioning between the members is an effective way to prevent cracking and, consequently, enhance the durability of the system. Furthermore, overlays are usually provided to protect the deck and, specifically, the reinforcing bars. Post-tensioning and overlaying could be seen as additional methods to improve the durability of the system. The inverted-tee system was conceived as a rapid construction system in which both post-tensioning and overlays at the top of the section were avoided to speed erection. Therefore, the problems anticipated in standard cast-in-place concrete slabs could be magnified.

For these reasons, studies on MN bridge 13004 and on laboratory specimens were continued after the conclusion of the initial study (Fig. 1).¹ These studies focused on the durability of the system related to joint cracking and the development of an accurate procedure to design the system for different span lengths and widths. This paper summarizes a preliminary study of various analysis and design aspects of the Minnesota inverted-tee system.

MN bridge 13004 in Center City was monitored since the deck was cast in September 2005. Because of joint cracking, three joints were instrumented at the midspan of the 27-ft-long (8.2 m) center span of the three-span bridge (22-ft-long [6.7 m] outer spans) to monitor the transverse strains in the cast-in-place concrete connection between the precast concrete sections, in the concrete over the web corners, and in the mild reinforcement that crossed above the joint between the precast concrete sections. In addition, strain gauges were placed on longitudinal mild reinforcement. The full-scale laboratory specimen was built in 2006 using the same design criteria adopted for MN bridge 13004. To achieve uniformity in data acquisition and to compare the data from the two specimens, the laboratory specimen was instrumented to monitor transverse and longitudinal strains in the concrete and in the steel. The instrumentation was installed at locations similar to those used for MN bridge 13004.

Initially, the objective of the field and experimental studies was to verify the continuity over the pier and the transverse load distribution related to traffic and environmental loads. Eventually, the investigation focused on the mechanism of transverse reflective cracking. This task was achieved by performing static truck tests in April 2007.

Development of the precast concrete inverted-tee slab system

Ralls^{2,3} investigated rapid construction techniques used for prefabricated bridges in France, Germany, and Japan. In particular, the Poutre-Dalle system used in France showed characteristics that make it suitable for the rapid replace-



Center City Bridge (MN bridge 13004)

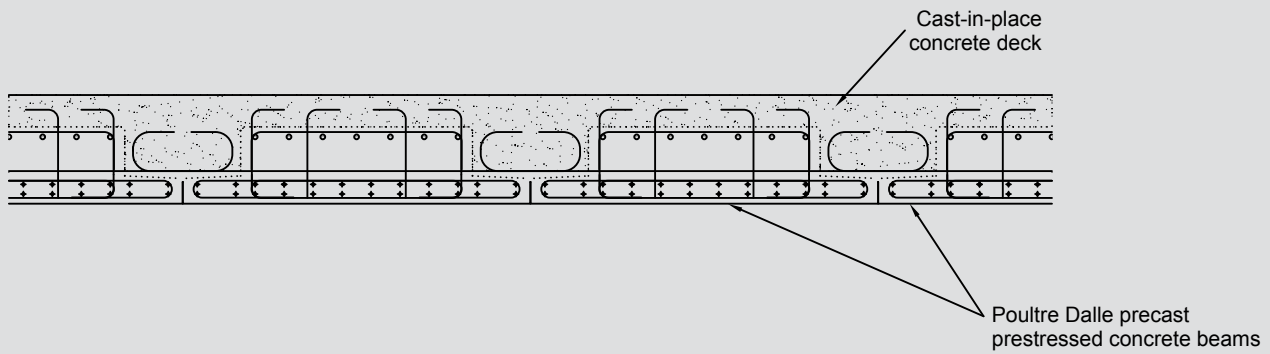


Laboratory specimen

Figure 1. Studies on the Center City Bridge and a laboratory specimen were conducted.

ment of short-span bridges (Fig. 2). Hagen⁴ used a preliminary and modified design procedure to build two bridges using the newly developed concept. The available literature on this system is limited.

The Poutre-Dalle concept arose from the desire to develop a fast and reliable concrete system to build and replace existing bridges. The geometry of the system and the pres-



Deck and connection reinforcement for typical Poutre Dalle systems



Minnesota inverted tee beam in precasting plant



Deck and connection reinforcement for University of Minnesota specimens

Figure 2. Precast concrete inverted-tee beam systems for bridges.

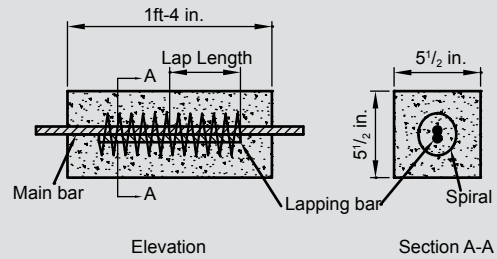
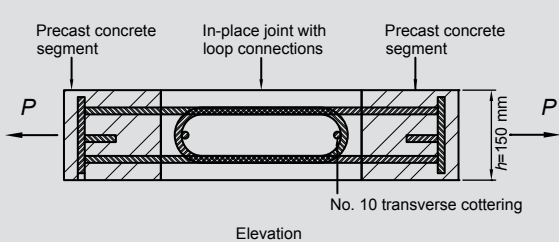
ence of a cast-in-place concrete deck seemed suited for a loop bar connection between panels. Loop bar reinforcing details in the cast-in-place concrete joint have been used in several applications involving the connection between precast concrete members. However, because the joint between precast concrete members is vulnerable to cracking, various studies have focused on crack control in the joint and on the use of either fiber reinforcement or higher-strength concrete. Tests in Japan and Korea also focused on the problem of the minimum radius of the looped bars in these connections. In these studies, the typical shear key connection detail⁵ was considered, in addition to looped bars,⁶⁻⁸ straight bars with spiral connection,⁹ headed bar connections,¹⁰ and welded connectors⁵ (**Fig. 3**).

The preliminary design of the Minnesota State Department of Transportation (MnDOT) precast concrete members was based on the cross section of a prefabricated standard I-beam (27M). The inverted-tee shape was defined considering a wider bottom flange (6 ft [1.8 m] instead of 4 ft [1.2 m]) and incorporating the top flanges into the cast-

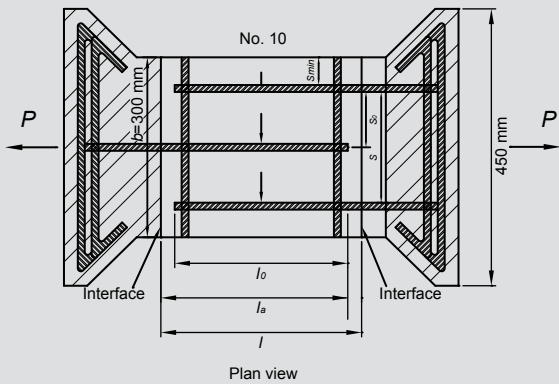
in-place concrete web. **Figure 4** represents the final cross section used to replace two bridges in the state.

Purpose of the study

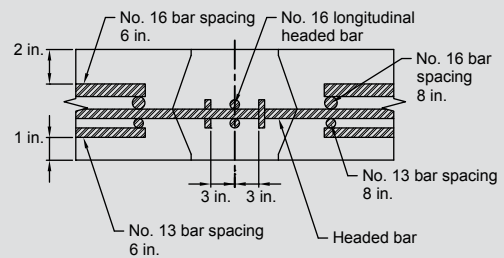
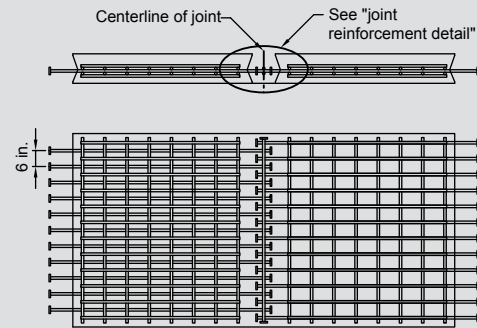
Although several bridges have been built using the inverted-tee system, there is still a lack of knowledge related to the optimum bridge configuration, maximum span length, and overall behavior of the system. In this paper, results from a series of parametric studies to determine the soundness of the preliminary design assumptions (stress limits) and the feasibility of the system are presented (that is, bridge configuration and weight of the section). In addition, the results from a series of linear elastic finite element models (FEMs) of MN bridge 13004 are documented. In this way, the results from the FEM could be compared with the truck test results to lend confidence to the modeling of the laboratory specimen. The verified model was used to investigate the stress concentrations at the joints between precast concrete panels that would initiate reflective cracking. Subsequent stages of this project¹ could also use the



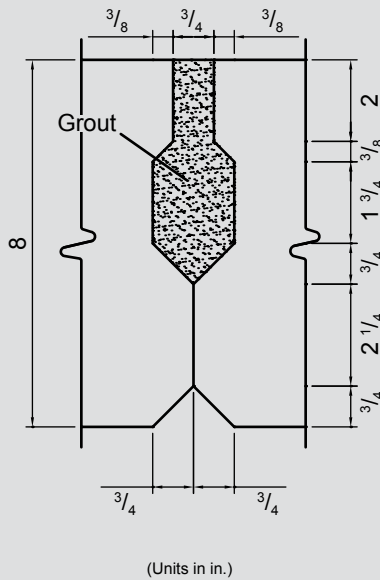
Straight bars with spiral connection.
Courtesy of Tadros, Einea, and Yehia, 1999.



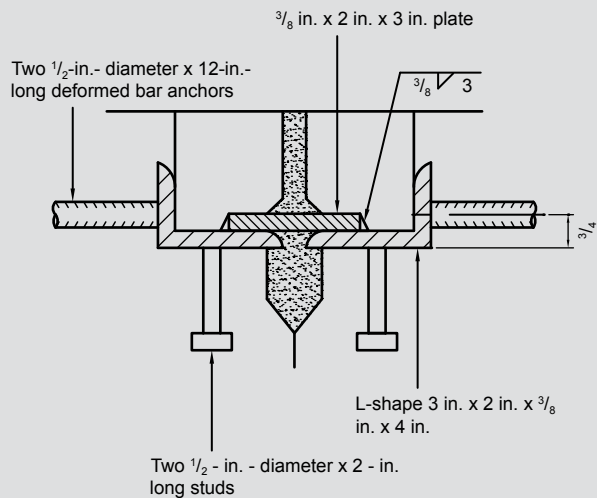
Tensile in place loop connections specimen with transverse bars. Courtesy of Tan, 1998.



Joint reinforcement detail
Headed bar connections.
Courtesy of Ma, Li, and Bateman, 2006.



Welded connector. Courtesy of Martin and Osborn, 1983.



Grouted shear key.
Courtesy of Martin and Osborn, 1983.

Figure 3. In addition to the typical shear key connection detail, looped bars, straight bars with spiral connection, headed bar connections, and welded connectors were considered. Note: b = length of joint; h = depth of section; l = width of joint; l_a = loop connection total transverse length; l_o = distance between centers of the loop connection reinforcing bars; P = load; s_{min} = distance between loop connection reinforcing bar and edge of joint; s_o = loop connection reinforcing bars spacing. 1 in. = 25.4 mm; 1 ft = 0.305 m.

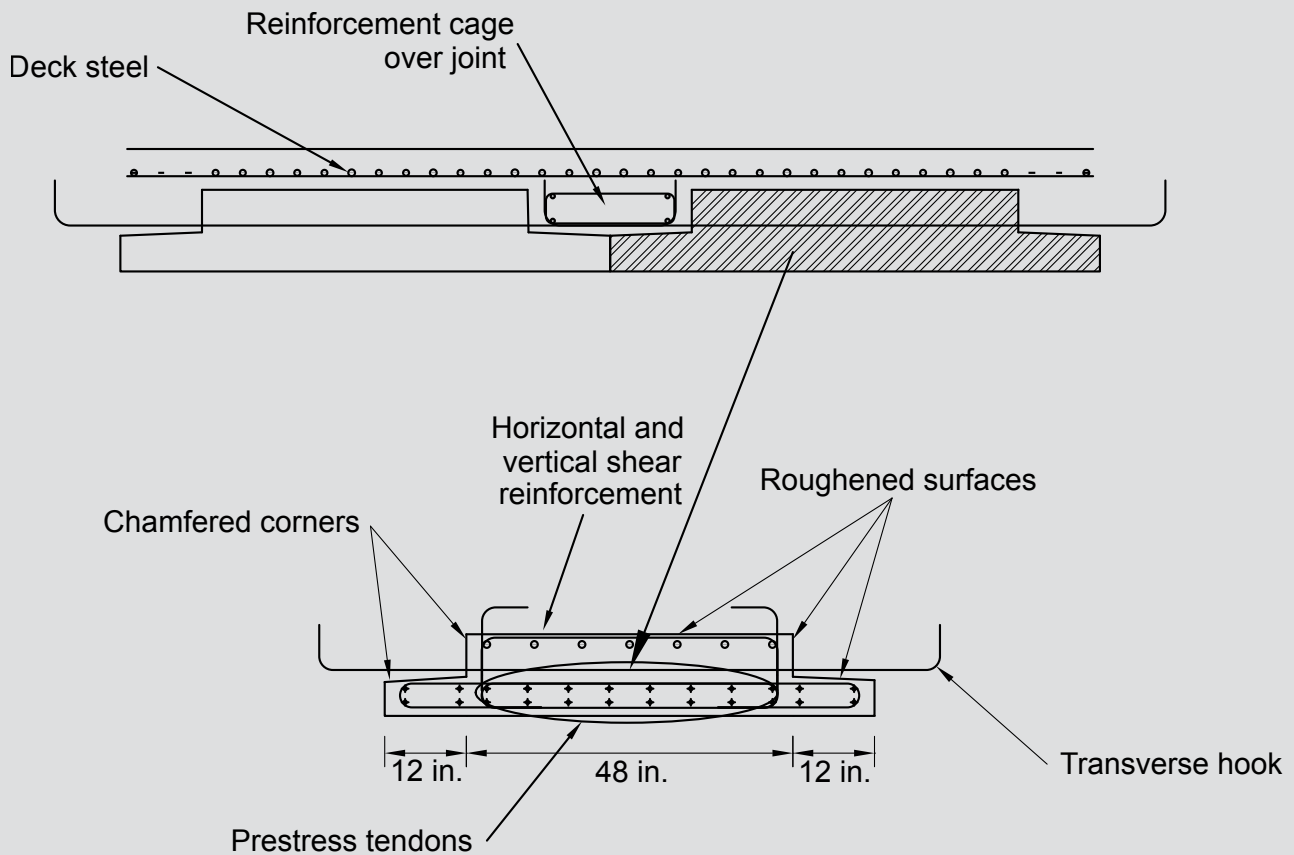


Figure 4. Conceptual cross section of Minnesota Department of Transportation's precast concrete slab-span system. Note: 1 in. = 25.4 mm.

calibrated model to investigate transverse load distribution or behavior of the system under fatigue loading and at failure.

Once the calibration of the model for MN bridge 13004 was completed, the FEM for the laboratory specimen could be designed based on analogous assumptions. Future phases of this research are expected to use the latter model to simulate static and fatigue load tests for the laboratory specimen.

Parametric study

A series of slab-span inverted-tee systems was selected for investigation to represent the range of spans for which the slab-span concept might be used. The selected systems were optimized using a preliminary design process similar to that followed by MnDOT for the design of composite slab-span bridges in Minnesota. Because of the preliminary nature of the study, the design process focused exclusively on maximum allowable stresses at release and in service. The shape of the cross section was kept constant; section depth, span length, bridge configurations, and number of prestress strands were varied. Based on MnDOT's experience in the construction of this type of bridge, some design parameters were kept constant: concrete compressive strength for the precast concrete $f'_{c_precast}$ and cast-in-place

concrete f'_{c_CIP} , flange thickness, flange width, overall section width, and thickness of cast-in-place concrete connection over the web. Strand patterns and overall section depths were determined to optimize the sections for the span lengths and configurations chosen.

Bridge configuration

Although MN bridge 13004 has 22 ft and 27 ft (6.7 m and 8.2 m) spans and the laboratory specimen has only two 22 ft spans, four span lengths were considered for the parametric study: 20 ft, 30 ft, 50 ft, and 65 ft (6.1 m, 9.1 m, 15.2 m, and 19.8 m). Thus, the parametric study compared different sections based on the bridge configurations in which physical measurements were being made. The 20-ft-long span was chosen to represent the shortest practicable span, the spans of 30 ft and 50 ft were chosen because of the broad applicability of the composite slab-span concept within this range, and the 65 ft span was chosen because it was thought to represent the maximum feasible span length for this system.

Information about bridge configurations employing the precast concrete composite slab-span system was provided by MnDOT. As a result, the following three-span configurations were selected for preliminary consideration: 20 ft-30 ft-20 ft

(6.1 m-9.1 m-6.1 m), 30 ft-50 ft-30 ft (9.1 m-15.2 m-9.1 m), and 50 ft-50 ft-50 ft (15.2 m-15.2 m-15.2 m). For a two-span bridge, a 50 ft-50 ft configuration would not be much different from the 30 ft-50 ft-30 ft system; therefore, a 65 ft-65 ft (19.8 m-19.8 m) two-span configuration was selected. This system was also thought to represent a reasonable configuration for an interstate overpass. Both two-span and three-span configurations were considered because MN bridge 13004 has three spans (22 ft, 27 ft, and 22 ft [6.7 m, 8.2 m, and 6.7 m]), while the laboratory specimen has two 22 ft spans.

While optimizing the composite slab-span configurations, the 65 ft (19.8 m) span length was found to be impractical; a 62 ft (18.9 m) span was substituted. The 62 ft span maintains the maximum allowed stresses and maximum depth and weight of the section below the specified limits. As a consequence, a three-span 45 ft-62 ft-45 ft (13.7 m-18.9 m-13.7 m) combination was considered. A 45 ft span was selected to replicate one of the two bridges built in Minnesota in 2005.

Bridge loading

Moment envelopes were developed for the three-span configurations using the American Association of State Highway and Transportation Officials' *AASHTO LRFD Bridge Design Specifications*¹¹ for load distribution factors. The moment envelopes were obtained using finite element software and were based on two moving-load situations (HL-93 and tandem vehicles) concurrently combined with a static, uniformly distributed load of 640 lb/ft (9340 N/m) along the entire length. A dynamic allowance factor equal to 0.33 was considered for the moving-load cases.

The load distribution factor used by MnDOT for MN bridge 13004 is not directly addressed for this system. In fact, none of the categories in AASHTO LRFD specifications section 4.6.2.2 considers the precast concrete slab-span system. Although the gap between flanges of adjacent precast concrete sections could reduce the transverse stiffness and cause the effective width to be smaller than that of a monolithic system, the equation for effective width of a monolithic concrete slab-type bridge given in AASHTO LRFD specifications section 4.6.2.3 was used for design (equivalent strip widths for slab-type bridges).

$$E = 84.0 + 1.44\sqrt{L_i W_1}$$

where

E = equivalent width, in.

L_i = modified span length taken equal to the lesser of the actual span or 60.0 ft (18.3 m)

W_1 = modified edge-to-edge width of bridge = 60.0 ft (18.3 m)

Restraint moments

In the initial design phase, restraint moments were assumed to be negligible, assuming the deck would be placed 90 days after the casting of the precast concrete sections.¹¹ In a second phase, restraint moments were considered for the configurations including 20 ft, 30 ft, 50 ft, and 65 ft spans (6.1 m, 9.1 m, 15.2 m, and 19.8 m) assuming 14 days for the age of the precast concrete at the time that continuity with the cast-in-place concrete was established. The restraint moments were calculated using the Portland Cement Association (PCA) method reported by Freyermuth.¹²

The PCA method is considered to predict accurate magnitudes for the maximum positive restraint moments for the time of continuity assumed in the calculations but can overestimate negative restraint moments. The method is based on both structural mechanics concepts and assumed creep and shrinkage data. It is different from the method reported by Oesterle et al.¹³ because of the way the diaphragm is modeled; the restraint of deck shrinkage is neglected, and the recommended creep and shrinkage coefficients are higher than American Concrete Institute's (ACI's) *Prediction of Creep, Shrinkage, and Temperature Effects in Concrete Structures*¹⁴ or AASHTO LRFD specifications coefficients for the same case. As a consequence, only the positive restraint moment case was considered because of its significant effect on the design and behavior of the system. The positive restraint moment increases the value of the positive midspan moment in service, while negative restraint moments increase the negative moment over the piers.¹⁵ In the latter case, it has been assumed that the top of the precast concrete section and the cast-in-place concrete will be provided with adequate bonded reinforcement to control cracking.

After the preliminary study was completed, subsequent investigation of the Minnesota inverted-tee system concluded that, due to the potential of thermal gradients to generate large restraint moments, bridges using precast concrete composite slab systems be designed as a series of simply supported spans.¹ In the remainder of this paper, however, continuity at the piers is assumed, because that condition was the initial basis for the Minnesota inverted-tee system.

Selection of parameters

The parameters were kept constant:

- flange thickness = 3 in. (75 mm)
- flange width protruding from each side of web = 12 in. (300 mm)
- overall width of the precast concrete section = 6 ft (1.8 m)

Table 1. Concrete stress limits for preliminary design

Transfer	Service
$f_{c_allow} = 0.6 f'_{ci} = 3 \text{ ksi}$	$f_{c_allow} = 0.45 f'_c = 2.7 \text{ ksi}$
$f_{t_allow} = 0.24 \sqrt{f'_{ci}} = 0.537 \text{ ksi}$	$f_{t_allow} = 0.19 \sqrt{f'_c} = 0.465 \text{ ksi}$
Note: f'_c = concrete specified compressive strength; f_{c_allow} = allowable compressive stress in concrete at transfer or under service loads; f'_{ci} = concrete compressive strength at release; f_{t_allow} = allowable tensile stress in concrete at transfer or under service loads. 1 ksi = 6.895 MPa.	

- thickness of cast-in-place concrete over precast concrete web = 6 in. (150 mm)
- compressive strength of cast-in-place concrete $f'_{c_CIP} = 4 \text{ ksi}$ (28 MPa)
- compressive strength of precast concrete $f'_{c_precast} = 5 \text{ ksi}$ (34 MPa) at transfer = 6 ksi (41 MPa) at 28 days

Minimizing the flange thickness was considered important to minimize the gap between adjacent flanges. A flange thickness of 3 in. (75 mm) allowed for proper cover to the reinforcement from the bottom surface and a sufficiently robust section to avoid damage during handling. The width of the flange was maintained at 12 in. (300 mm) to provide sufficient room to develop the reinforcement across the interface through the cast-in-place concrete section between the precast concrete webs. The overall width of 6 ft (1.8 m) for the precast concrete section was chosen as a reasonable dimension for shipping and handling.

The 6 in. (150 mm) thickness of the cast-in-place concrete over the web provided 3 in. (75 mm) of cover over the deck reinforcement while accommodating a reasonable depth of concrete to place the longitudinal and transverse deck reinforcement with sufficient clearance over the precast concrete web. For longer spans, deeper precast concrete sections allowed the 6 in. (150 mm) depth of cast-in-place concrete over the precast concrete web to remain constant. The nominal compressive strengths of the precast concrete section at transfer and service, as well as the cast-in-place concrete compressive strengths, were deemed to be typical. In optimizing the cross sections, slight increases in concrete compressive strengths of the precast concrete section were identified where appropriate.

Concrete stress limits

Considering the listed assumptions for nominal precast concrete strengths, the stress limits at transfer and service were determined according to the AASHTO LRFD specifications (Table 1).

Values of the stresses at the ends and at midspan were considered for both transfer and service. Stress limits were selected according to Table 3.4.1-1 of the AASHTO LRFD specifications, checking the behavior of the section at service stages I-II and III. The stresses associated with supporting the freshly cast concrete before developing composite action were also considered. The stresses at the ends at transfer and in service were calculated at the end of each beam, neglecting the effect of the tendon transfer length. In addition, the ultimate strength of the composite section was evaluated for flexure and shear.

Prestress losses

Prestressing losses were calculated using the method proposed by Zia et al.¹⁶ The prestressing strands were assumed to be low-relaxation, 1/2-in.-diameter (13 mm), Grade 270 (1860 MPa) strands jacked to an initial value of 75% of f_{pu} (where f_{pu} is the specified tensile strength of prestressing tendons) or 202.5 ksi (1396 MPa). The equality of modular ratios for the precast concrete section n_s and cast-in-place concrete deck n_d justified ignoring the potential stiffness provided to the section by the deck reinforcement.

$$n_s = \frac{E_{steel}}{E_{precast}} = n_d = \frac{E_{steel}}{E_{deck}}$$

where

E_{deck} = modulus of elasticity of deck cast-in-place concrete

$E_{precast}$ = modulus of elasticity of precast concrete

E_{steel} = modulus of elasticity of steel

Results from parametric study

Optimized sections

As previously mentioned, this investigation was limited to the effects of section depth, span length, bridge configuration, and prestress force on the preliminary design of this type of system. For a given bridge configuration and span length, an optimum section depth and prestress force were calibrated (or vice versa). This optimization process was governed by the maximum allowable design stresses at release and in service. No shear design or detailing or behavior at ultimate was taken into account.

Table 2 shows the optimized section results for the span lengths investigated. While the span lengths were kept constant, the optimized sections varied slightly according to the bridge configuration. For brevity, Table 2 lists the sections that required the most strands to meet the stress limit requirements. For each optimized section, the table

Table 2. Results from the parametric study for optimized section design

Parameter	Span length					
	20 ft	30 ft	45 ft	50 ft	62 ft	65 ft
Total depth of section, in.	14	16	20	22	26	28
L/h	17	23	27	27	28.6	28
Number of strands	12	16	36	38	46	54
Total prestress force at jacking, kip	371	495	1114	1175	1031	1670
Total prestress force after losses, kip	317	421	880	939	1080	1327
f_{t_top} at release at ends, ksi	n.a.	n.a.	0.81	0.93	1.1	1.14
f_{c_bottom} at release at ends, ksi	n.a.	n.a.	3.3	3.22	3.38	3.59
f_{c_top} at service at midspan, ksi	1.05	1.58	2.4	2.36	2.59	2.61
f_{t_bottom} at service at midspan, ksi	0.42	0.39	0.38	0.41	0.46	0.41
Weight of precast concrete section, kip	9.5	17.5	34.9	43.8	66.7	76.4

Note: f_{c_bottom} = compressive stress in bottom fiber; f_{c_top} = compressive stress in top fiber; f_{t_bottom} = tensile stress in bottom fiber; f_{t_top} = tensile stress in top fiber; h = depth of section; L = length of unsupported span; n.a. = not applicable. 1 in. = 25.4 mm; 1 ft = 0.305 m; 1 kip = 4.44 kN; 1 ksi = 6.895 MPa.

summarizes the total composite section depth, span-to-depth ratio L/h , required number of strands to meet the release and service stress limits, total prestress force assumed at jacking and transfer, stresses at transfer and service, and weight of the precast concrete section.

For span lengths exceeding 45 ft (13.7 m), the stresses at transfer exceeded the AASHTO LRFD specifications limits. In these instances, it was assumed that mild reinforcement would be used at the top of the section to meet the tension stress limit requirements and the concrete compressive strength at release would be increased to meet the compressive stress limit requirements. The stresses obtained at service are also listed; these determined the design requirements for the sections.

The design of the inverted-tee system was governed by the stress limits at the ends at transfer and at midspan in service. While the bottom fiber tension stress limits controlled

in service in most cases, the tension limit for the top fiber at the ends at transfer should not be an issue because it is possible to add mild longitudinal reinforcement to carry the required tension force.

Optimized sections by span length for various bridge configurations

Tables 3 through 9 summarize the results obtained from the parametric study. Each table represents a specific bridge configuration, and the optimization of the section for each span is shown (for example, the 20 ft-30 ft-20 ft [6.1 m-9.1 m-6.1 m] configuration has an optimized section for the 20 ft span and the 30 ft span). The material in the tables is presented in the following manner:

- For each span length, optimized sections are presented in terms of the required beam depth and associated number of tendons.

Table 3. Span length optimization of a 20 ft-30 ft-20 ft span bridge

Physical characteristics	Span length, ft	20	20	30	30
	Precast concrete depth, in.	8	8	10	10
	Number of tendons	8	10	14	16
Service stresses exceeding the limits, ksi (solution)	End, top	n.a.	n.a.	$f_t = 0.533$	$f_t = 0.582$ (four no. 5 bars)
	Midspan, bottom	$f_t = 0.667$	n.a.	$f_t = 0.514$	n.a.

Note: f_t = tensile stress; n.a. = not applicable (no problems encountered in satisfying stress limits). No. 5 = 16M; 1 in. = 25.4 mm; 1 ft = 0.305 m; 1 ksi = 6.895 MPa.

Table 4. Span length optimization of a 20 ft-50 ft-20 ft span bridge

Physical characteristics	Span length, ft	20	20	20	50	50
	Precast concrete depth, in.	8	8	10	14	16
	Number of tendons	10	12	8	40	32
Release stresses exceeding the limits, ksi (solution)	End, top	n.a.	n.a.	n.a.	$f_t = 0.819$	$f_t = 0.88$ (nine no. 5 bars)
	End, bottom	n.a.	n.a.	n.a.	$f_c = 3.54, f'_{ci} = 5.9$	n.a.
Service stresses exceeding the limits, ksi (solution)	End, top	n.a.	n.a.	n.a.	$f_t = 0.999$	$f_t = 1.054$ (eight no. 6 bars)
	Midspan, top	n.a.	n.a.	n.a.	$f_c = 2.835, f'_c = 6.3$	n.a.
	Midspan, bottom	$f_t = 0.631$	n.a.	n.a.	n.a.	n.a.

Note: f_c = compressive stress; f'_c = design concrete compressive strength in service; f'_{ci} = concrete compressive strength at release; f_t = tensile stress; n.a. = not applicable (no problems encountered in satisfying stress limits). No. 5 = 16M; no. 6 = 19M; 1 in. = 25.4 mm; 1 ft = 0.305 m; 1 ksi = 6.895 MPa.

Table 5. Span length optimization of a 30 ft-50 ft-30 ft span bridge

Physical characteristics	Span length, ft	30	30	50
	Precast concrete depth, in.	8	10	16
	Number of tendons	22	16	32
Release stresses exceeding the limits, ksi (solution)	End, top	n.a.	n.a.	$f_t = 0.882$ (nine no. 5 bars)
Service stresses exceeding the limits, ksi (solution)	End, top	$f_t = 0.481$ (two no. 5 bars)	$f_t = 0.6$ (four no. 5 bars)	$f_t = 1.037$ (eight no. 6 bars)
	Midspan, bottom	$f_t = 0.631$	n.a.	n.a.

Note: f_t = tensile stress; n.a. = not applicable (no problems encountered in satisfying stress limits). No. 5 = 16M; no. 6 = 19M; 1 in. = 25.4 mm; 1 ft = 0.305 m; 1 ksi = 6.895 MPa.

Table 6. Span length optimization of a 50 ft-50 ft-50 ft span bridge

Physical characteristics	Span length, ft	50	50
	Precast concrete depth, in.	16	18
	Number of tendons	38	32
Release stresses exceeding the limits, ksi (solution)	End, top	$f_t = 0.928$ (nine no. 5 bars)	$f_t = 0.907$ (eight no. 6 bars)
	End, bottom	$f_c = 3.22, f'_{ci} = 5.4$	n.a.
Service stresses exceeding the limits, ksi (solution)	End, top	$f_t = 1.107$ (eight no. 6 bars)	$f_t = 1.08$ (ten no. 6 bars)

Note: f_c = compressive stress; f'_{ci} = concrete compressive strength at release; f_t = tensile stress; n.a. = not applicable (no problems encountered in satisfying stress limits). No. 5 = 16M; no. 6 = 19M; 1 in. = 25.4 mm; 1 ft = 0.305 m; 1 ksi = 6.895 MPa.

- Stresses exceeding the limits are listed for each case in ksi, with compressive stresses represented by f_c and tensile stresses represented by f_t .
- Stresses exceeding the limits are followed by proposed solutions, either an increased section depth or an increased number of strands. Where it was deemed reasonable to add tension reinforcement or to increase the concrete compressive strength, the solution is expressed

Table 7. Span length optimization of a 62 ft-62 ft span bridge

Physical characteristics	Span length, ft	62	62
	Precast concrete depth, in.	20	22
	Number of tendons	52	46
Release stresses exceeding the limits, ksi (solution)	End, top	$f_t = 1.085$ (ten no. 6 bars)	$f_t = 1.11$ (twelve no. 6 bars)
	End, bottom	$f_t = 1.259$ (twelve no. 6 bars)	$f_c = 4.14, f'_{ci} = 6.9$
Service stresses exceeding the limits, ksi (solution)	End, top	$f_t = 1.259$ (twelve no. 6 bars)	$f_t = 1.268$ (eight no. 8 bars)

Note: f_c = compressive stress; f'_{ci} = concrete compressive strength at release; f_t = tensile stress; n.a. = not applicable (no problems encountered in satisfying stress limits). No. 5 = 16M; no. 6 = 19M. 1 in. = 25.4 mm; 1 ft = 0.305 m; 1 ksi = 6.895 MPa.

Table 8. Span length optimization of a 45 ft-62 ft-45 ft span bridge

Physical characteristics	Span length, ft	45	45	62	62
	Precast concrete depth, in.	14	16	18	20
	Number of tendons	36	28	56	46
Release stresses exceeding the limits, ksi (solution)	End, top	$f_t = 0.812$ (six no. 5 bars)	$f_t = 0.845$ (nine no. 5 bars)	$f_t = 0.972$	$f_t = 1.234$ (twelve no. 6 bars)
	End, bottom	$f_c = 3.24, f'_{ci} = 5.4$	n.a.	$f_c = 3.087\text{m}, f'_c = 6.86$	n.a.
Service stresses exceeding the limits, ksi (solution)	End, top	$f_t = 1.076$ (nine no. 5 bars)	$f_t = 1.099$ (nine no. 6 bars)	$f_t = 1.076$	$f_t = 1.234$ (twelve no. 6 bars)
	Midspan, top	n.a.	n.a.	$f_c = 3.087, f'_c = 6.86$	n.a.

Note: f_c = compressive stress; f'_c = design concrete compressive strength in service; f'_{ci} = concrete compressive strength at release; f_t = tensile stress; n.a. = not applicable (no problems encountered in satisfying stress limits). No. 5 = 16M; no. 6 = 19M; 1 in. = 25.4 mm; 1 ft = 0.305 m; 1 ksi = 6.895 MPa.

as such. Where tension stresses exceed the limits, the solution is expressed as the number of longitudinal bars required to carry the entire tensile force applied at the top of the section. In cases where compressive stresses exceed the limits, the solution is expressed as an increased concrete compressive strength to address the limits (f'_{ci} at release and f'_c in service).

Summary

Stress limits in service controlled the design of the 20 ft (6.1 m) spans (Tables 3 and 4). For an 8-in.-deep (200 mm) precast concrete section, eight strands were not sufficient for either of the configurations analyzed (20 ft-30 ft-20 ft and 20 ft-50 ft-20 ft [6.1 m-9.1 m-6.1 m and 6.1 m-15.2 m-6.1 m]). Increasing the number of tendons from 8 to 10 made it possible to satisfy the tension limit stress at service for the 20 ft-30 ft-20 ft configuration. For the 20 ft-50 ft-20 ft configuration, it was necessary to use 12 tendons. Alternatively, the depth of the section could be

increased from 8 in. to 10 in. (200 mm to 250 mm) using 8 tendons. All other stress limits were satisfied. Considering the effects of the positive restraint moment, it was necessary to increase the number of tendons from 10 to 16 for the 20 ft-30 ft-20 ft configuration and from 12 to 18 for the 20 ft-50 ft-20 ft configuration. With the same section geometry, all stress limits were satisfied.

For the 30 ft (9.1 m) span, in both the 20 ft-30 ft-20 ft (6.1 m-9.1 m-6.1 m) and the 30 ft-50 ft-30 ft (9.1 m-15.2 m-9.1 m) configurations (Tables 4 and 5), a 10-in.-deep (250 mm) precast concrete section with 16 prestressing tendons was required to satisfy the stress limits in service. In considering the effect of the positive restraint moment, the prestressing force had to be increased to satisfy the stress limits.

For the 45 ft (13.7 m) span, the precast concrete section was optimized for a 14 in. (360 mm) depth (Table 8) with a reasonable amount of prestressing force and weight limited to less than 40 kip (180 kN).

Table 9. Span length optimization of a 65 ft-65 ft span

Physical characteristics	Span length, ft	65	65
	Precast concrete depth, in.	20	22
	Number of tendons	62	54
Release stresses exceeding the limits, ksi (solution)	End, top	$f_t = 1.073$ (twelve no. 6 bars)	$f_t = 1.135$ (twelve no. 6 bars)
	End, bottom	$f_c = 4.116$, $f'_{ci} = 6.86$	$f_c = 3.6$, $f'_{ci} = 6$
Service stresses exceeding the limits, ksi (solution)	End, top	$f_t = 1.252$ (eight no. 8 bars)	$f_t = 1.296$ (ten no. 6 bars)
	Midspan, top	$f_c = 3.15$, $f'_c = 7$	n.a.

Note: f_c = compressive stress; f'_c = design concrete compressive strength in service; f'_{ci} = concrete compressive strength at release; f_t = tensile stress; n.a. = not applicable (no problems encountered in satisfying stress limits). No. 6 = 19M; no. 8 = 25M; 1 in. = 25.4 mm; 1 ft = 0.305 m; 1 ksi = 6.895 MPa.

Table 10. Final values for transverse stresses above the gap

Configuration	Transverse stress above crack, psi				
22-22, two beams wide	n.a.	n.a.	94	93.5	93.3
22-22, thirteen beams wide	n.a.	109	n.a.	108.5	n.a.
Mesh size, in.	6 × 6 × 6	5 × 5 × 5	4 × 4 × 4	3 × 3 × 3	2 × 2 × 2

Note: n.a. = not applicable. 1 in. = 25.4 mm; 1 psi = 6.895 kPa.

For the 50 ft (15.2 m) span, in both the 20 ft-50 ft-20 ft (6.1 m-15.2 m-6.1 m) (Table 4) and the 30 ft-50 ft-30 ft (9.1 m-15.2 m-9.1 m) (Table 5) configuration cases, a 16-in.-deep (400 mm) precast concrete section with 32 prestressing tendons was required to satisfy the stress limits at service. In addition, mild reinforcement was required for the tension stress at the ends at the top. For the 50 ft-50 ft-50 ft configuration (Table 6), additional prestressing tendons had to be added (38 total). In considering the effects of the positive restraint moment, the prestressing force or the depth of the precast concrete section needed to be increased.

For the 65 ft (19.8 m) span in the 65 ft-65 ft configuration (Table 9), a minimum depth of 20 in. (510 mm) was necessary. The required three rows of tendons resulted in excessive compressive stress at the ends at release and at midspan in service. Using a 22-in.-deep (560 mm) precast concrete section with 54 tendons required a concrete compressive strength at transfer of 6 ksi (41 MPa) rather than the nominal value of 5 ksi (34 MPa). Using a 24-in.-deep (610 mm) precast concrete section with 46 prestressing tendons solved the problem, but with this depth the weight of the precast concrete section exceeded 80 kip (360 kN), which could make transport difficult. As for the previous cases, when the positive restraint moment was considered, the prestressing force needed to be increased. However, no changes in the section properties were required.

Because of the difficulties encountered with the 65 ft (19.8 m) span, a 62 ft (18.9 m) span was selected as an upper bound. This allowed a decrease in section depth (Tables 7 and 8), prestress force, and weight. The weight was confined to less than 70 kip (310 kN) and the precast concrete section depth to 20 in. (500 mm).

Finite element model

This section describes the preliminary finite element study of the potential system weaknesses that are not addressed by the preliminary design.

Finite element software was used to conduct this numerical study. The calibration of the FEM of MN bridge 13004 was based mainly on the longitudinal and transverse strains measured during the static truck test conducted in April 2007.¹

The concrete was modeled using eight-node, solid, quadratic, three-dimensional (that is, brick) stress elements. Reduced integration was used for all of the analyses. The model was based on the simplified assumption of purely elastic behavior of the materials because of the low magnitude of the strains measured during the truck test. Two different materials and geometric properties were considered for the precast concrete beams and the deck. As purely isotropic elastic materials, they were defined through their Young's moduli and Poisson's ratios.

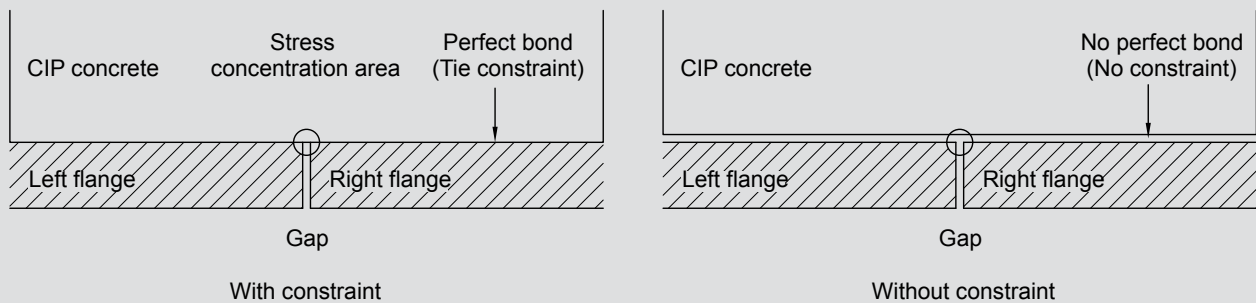


Figure 5. Detail of the gap between precast concrete beams and deck. Note: CIP = cast-in-place.

The gap between the adjacent flanges of the precast concrete beams was modeled assuming contact between hard, frictionless surfaces. The initial gap opening between the lateral flanges of the beams was assumed to be equal to zero. To connect the deck to the beams, a tie constraint was used between the two surfaces. This contact representation between the cast-in-place concrete deck and precast concrete beams was deemed efficient because the fresh concrete placed directly on the surface of the precast concrete beams was assumed to establish perfect bond and because of the presence of 12-in.-spaced (300 mm) stirrups coming out of the top surface of the precast concrete members. In fact, if the friction and the bond between the two different types of concrete were not perfect, the presence of a minimum number of stirrups to satisfy horizontal shear requirements for the composite section would guarantee the conditions for monolithic structural behavior.

To model the reinforcement, linear three-dimensional truss elements were considered. The truss elements were embedded in the solid concrete elements assuming perfect bond. The reinforcement configuration was based on the nominal configuration of the steel reinforcement obtained from the MnDOT design drawings for MN bridge 13004.

Gap representation between precast concrete elements

During the preliminary analysis, the stresses at the bottom of the cast-in-place concrete became unbounded during the remeshing process as the element size was decreased. This gap represents a discontinuity that generates a stress concentration where stresses increase to infinity with distance r from the discontinuity. Although this gap does not resemble a crack, it represents a singularity, like sharp corners, notches, or convex interfacial joints, and gives rise to reflective cracking.

Two FEMs were used to investigate the effect of the gap: a preliminary model of the laboratory specimen and an extension of it in which the width was extended from 2 to 13 beams. The load applied was a uniform pressure on a patch area corresponding to the size of a truck wheel (20 in. \times 10 in. [500 mm \times 250 mm]). Considering the gap as a

mathematical crack, it was assumed that the flanges of the beam could separate from the deck, so the tie constraint between the deck surface and the surface of the beam above the joint was removed. In this manner, the continuity of the system between crack and deck was avoided and the deck was considered to act as a continuous separate unit above the gap (Fig. 5).

The assumption regarding the constraint between the deck and the precast concrete beams at the gap proved to be sound (Table 10). Clearly, refining the mesh size did not lead to unbounded values for the transverse stresses and provided a converging solution as element size was reduced for both model widths.

To lend more confidence to the analytical results, a second approach was developed. A layer of an idealized soft plastic material was introduced between the deck and the top of the discontinuity in the FEM. The material was modeled using an elastic–perfectly plastic stress-strain law with a low yield stress. Young’s modulus was taken as 1 ksi (7 MPa) and the yield stress as 0.1 ksi (0.7 MPa). The transverse stress results were similar to those of the first approach or, at worst, within a few percentage points.

In the subsequent models, the first approach was considered accurate enough and less time consuming than the second one. For this reason, all of the FEMs described herein followed the assumptions described previously for the first approach.

MN bridge 13004 model

The FEM of MN bridge 13004 was developed for the entire bridge, which has spans of 22 ft, 27 ft, and 22 ft (6.7 m, 8.2 m, and 6.7 m).

Results for MN bridge 13004 model In the FEM model, the loads represented the rear tandem of an HS-20 truck.¹¹ Four patches were considered to model the actual tire positions measured during the field tests. Results of two of the tests were compared with the FEMs. In both cases, the front-axle loads were not included in the model because they

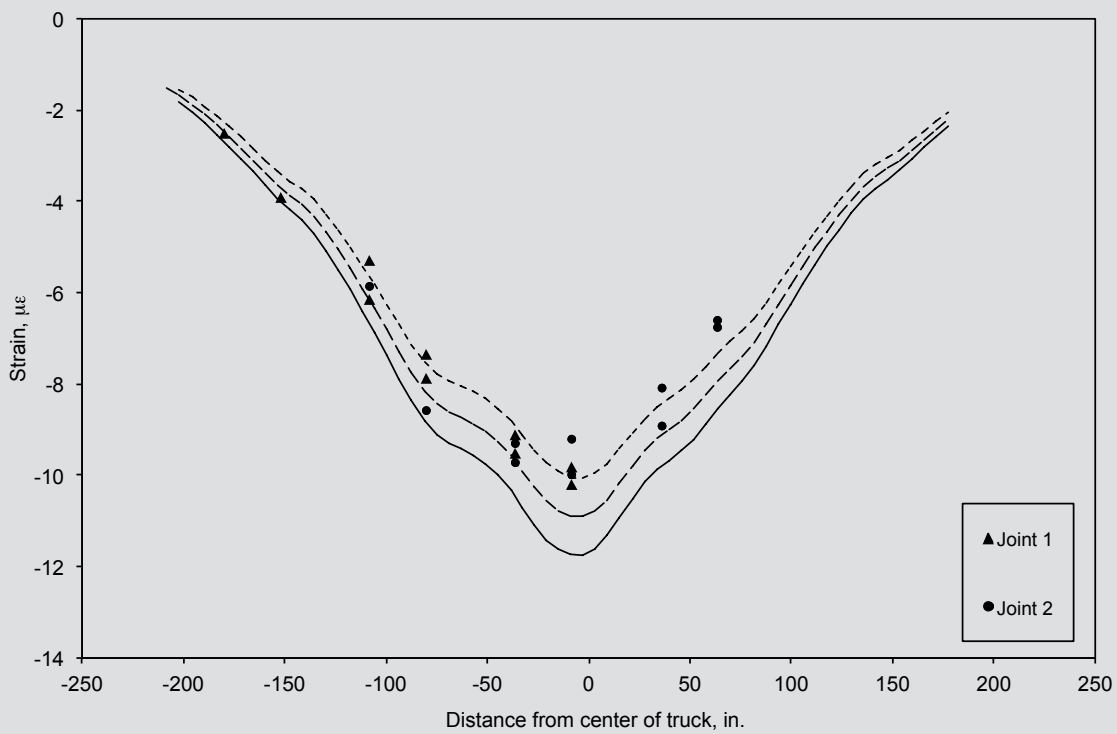
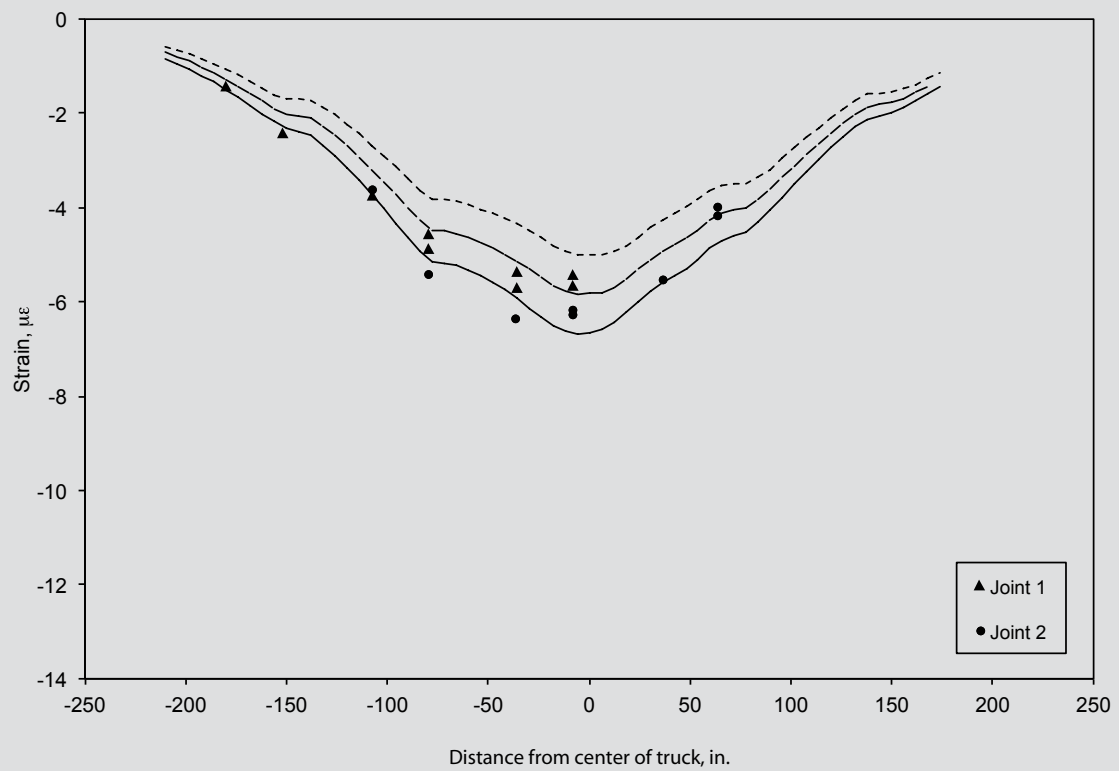


Figure 6. Comparison between truck test longitudinal strains and finite element model. Note: 1 in. = 25.4 mm.

were located directly over the pier; only the rear tandem loads were considered. The clear distance from pier to pier was modeled using two reaction lines to represent the edges of the support along each face of the pier.

Strains were identified in the FEMs corresponding to the locations of the strain gauges in MN bridge 13004. This facilitated comparison of the FEM results to the field data. The longitudinal strain gauges available in the cast-in-place concrete portion of the deck were positioned at three different depths between the precast concrete webs—9 in., 12.5 in., and 15.5 in. (230 mm, 320 mm, and 390 mm)—from the bottom of the composite section (the total depth of the composite slab-span section was 18 in. [460 mm]). The measurements from the gauges at 9 in. (230 mm) were not considered reliable because the measurements contained a significant amount of electrical noise. For this reason, only those at 12.5 in. and 15.5 in. (320 mm and 390 mm) were used to calibrate the FEM.

Only readings from two of the three joints of the bridge were considered to define the longitudinal strains. In fact, readings from the instrumentation in the transverse direction on one of the joints indicated the presence of a crack before the truck test was conducted. Due to the pure elastic behavior assumed for the materials, this joint and its behavior were clearly not modeled to represent such cracking behavior. However, readings from the two remaining instrumented joints (joints 1 and 2) were considered.

In **Fig. 6**, the longitudinal strains for the two joints investigated are compared with the results obtained from the FEMs for different cross-section depths. In the FEMs, the position of the truck tandem was centered above joint 1, with the wheels of the tandem positioned above the two adjacent webs (truck centered over the joint). As stated, the effect of the front axle was ignored because its wheels were located over the pier. In the plot, the symbols represent the measured data (joints 1 and 2) plotted at locations corresponding to the measured lateral distances of the strain gauges relative to the truck loads. Symmetry in behavior was assumed in completing the FEMs and plotting the results such that although the model represented the results for a single load case with the truck centered above joint 1, it was assumed that the same numerical results would be obtained across the width of the bridge if the truck had been centered above joint 2. Thus, **Fig. 6** shows that the largest strains in both joints 1 and 2 occur when the truck is centered over the joint. The nominal location of the gauges was 12.5 in. and 15.5 in. (320 mm and 390 mm) above the bottom of the composite section. The three lines plotted for the FEM at 12.5 in. and ± 0.5 in. (320 mm and ± 13 mm) and at 15.5 in. ± 0.5 in. (390 mm ± 13 mm) represent the potential variation in the vertical position of the gauges. These three lines can also be used to indicate the strain gradient in the section.

Figure 7 shows the results for transverse strains. The data from the test indicated that joint 1 seemed to be cracked in the transverse direction (nonsymmetric behavior of the transverse strains with respect to the center of the joint). Because the model investigated was elastic, only the uncracked joint 2 was considered. The transverse strain behavior for that case seemed to be close to the data. The strains in **Fig. 7** were determined between the precast concrete webs and 8.5 in. (220 mm) above the bottom of the section. Seeking the most relevant loading condition, only the test in which the wheels of the truck were located directly above two consecutive joints was used to evaluate the behavior of the transverse strains. In the plot, the solid line with symbols shows the behavior of the transverse strains obtained across the width of the joint from the FEM. The two thinner lines represent the measured values from the instrumentation for the two tests considered. Because the strain gauges had a gauge length of 6 in. (150 mm), the values from the FEM were averaged over 6 in. (150 mm) and plotted relative to the center of the strain gauge position (dashed line). Although the FEM output shows symmetry between one side of the joint and the other while the measured behavior did not appear to be symmetric, the model seems to closely simulate the magnitude and relative distribution of strains measured in the field.

Conclusion

In a parametric study, for all of the cases reported here, the service stresses were found to control the design. In particular, either the number of tendons or the depth of the section had to be increased to satisfy the bottom-fiber tensile stress limits in service. An increase in span length necessitated a larger number of tendons. When this was not feasible, the depth of the section was increased. Positive restraint moments increased the total positive moment at midspan, necessitating an increase in the prestress force for the same section.

The total weight of the precast concrete element may be limited by truck load limits or by crane capacity. For the truck load limits, elements should be limited to 80 kip (360 kN) without requiring a special permit. Typical cranes can readily handle 80 kip loads and even up to 130 kip (580 kN) in some cases. Further investigations regarding skewed configurations and economic feasibility of system configurations should be conducted. It appears that for sections deeper than the 25 in. (640 mm) needed for the for 62 ft (18.9 m) and 65 ft (19.8 m) spans, standardized I-sections might be more economical (practical).

Linear elastic FEMs were developed to simulate the behavior of a bridge in service, MN bridge 13004, and to design the static and fatigue tests of a similar laboratory specimen. The results from experimental tests and FEMs were in good agreement. The modeling assumptions can be considered acceptable for the purposes used here.

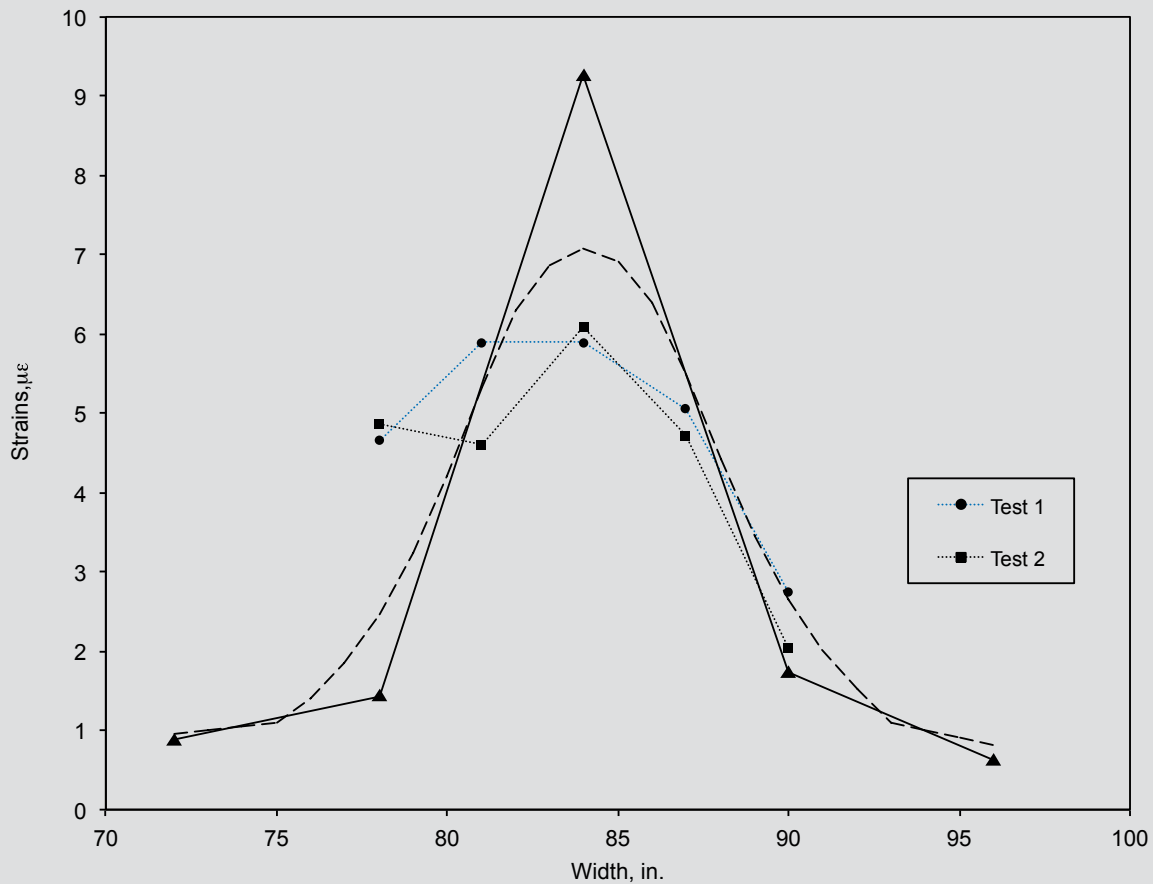


Figure 7. Comparison between truck test transverse strains and finite element model at 8.5 in. from the bottom of the section for joint 2. Note: The solid line is connecting the nodal values from the finite element analysis. The dashed line is connecting these nodal values averaged along the strain gauge length (6 in.). 1 in. = 25.4 mm.

Furthermore, the presence of shear reinforcement and the placement of the cast-in-place concrete can be assumed to guarantee adequate composite action between the members of the system. For the FEMs, tie constraint between precast concrete and cast-in-place concrete proved to be a reasonable assumption. More experimental results should be considered to determine the soundness of these linear elastic models. It is clear that they represent an acceptable assumption for this system when subjected to a certain range of service-load conditions.

Bursting reinforcement and environmental effects were not considered in this study and were subsequently investigated.¹ However, from field observations and FEMs of MN bridge 13004, the system has been shown to be reliable and stiff for normal and heavy traffic loads. Further investigations and calibration of the design process should take into account material nonlinearities as well as procedures to improve the thermal and shrinkage restraint analysis. The information here represents a solid base for further research and development of the inverted-tee system.

Acknowledgments

The research described in this paper was supported by the Department of Civil Engineering at the University of Minnesota. This support is gratefully acknowledged. Personnel of the MnDOT Office of Bridges and Structures provided technical expertise, especially Dan Dorgan, Keith Molnau, and Kevin Hagen, who are greatly thanked for their continuous and valuable feedback and support. The authors also extend their gratitude to J. Ma, professor at University of Tennessee–Knoxville; Roy Eriksson of Eriksson Technologies Inc.; Lee Marsh of Berger/ABAM Engineers Inc.; Stephen Seguirant of Concrete Technology Corp.; Chuck Prussack of Central Pre-Mix Prestress Co.; Matthew Smith of Meyer Borgman Johnson; Whitney Eriksson of Braun Intertec Corp.; and Holly Martell of Hilti Inc.

References

- French, C. E., C. K. Shield, D. Klaseus, M. Smith, W. Eriksson, Z. J. Ma, P. Zhu, S. Lewis, and C. E. Chapman. 2011. *Cast-in-Place Concrete Connections for Precast Deck Systems*. NCHRP Web-Only Document 173. Washington, DC: Transportation Research Board.
- Ralls, M. L. 2004. Prefabricated Bridges—Current U.S. Practice and Issues. Paper presented at FHWA/AASHTO Second National Prefabricated Bridge Elements and Systems Workshop, New Brunswick, NJ, September 8–10, 2004.
- Ralls, M. L. 2005. *Prefabricated Bridge Elements and Systems in Japan and Europe*. Federal Highway Administration report no. FHWA-PL-05-003. Washington, DC: American Association of State Highway and Transportation Officials.
- Hagen, K., S. Ellis, J. Fishbein, K. Molnau, E. Wolhowe, and D. Dorgan. 2005. Development and Construction of a Precast Inverted T System for Expediting Minnesota Slab Span Bridge Projects. *PCI National Bridge Conference*, Palm Springs, CA.
- Martin, L. D., and A. E. N. Osborn. 1983. *Connections for Modular Precast Concrete Bridge Decks*. Report no. FHWA/RD-82/106. Washington DC: Federal Highway Administration.
- Ryu, H. K., S. P. Chang, Y. J. Kim, and B. S. Kim. 2005. Crack Control of a Steel and Concrete Composite Plate Girder with Prefabricated Slabs under Hogging Moments. *Engineering Structures*, V. 27, No. 11 (September): pp. 1613–1624.
- Tan, C. K. 1998. Loop Connections for Precast Components. Bachelor's thesis, Department of Civil Engineering, National University of Singapore.
- Yeo, S. A. 1999. Loop Connections for Precast Components. Bachelor's thesis, Department of Civil Engineering, National University of Singapore.
- Tadros, M. K., A. Einea, and S. Yehia. 1999. Lap Splices in Confined Concrete. *Journal of the American Concrete Institute*, V. 96, No. 6 (November–December): pp. 947–955.
- Ma, Z. J., L. Li, and A. Bateman. 2006. Longitudinal Joint Details for Decked Bulb-Tee Girder Bridges. In *The PCI National Bridge Conference: Proceedings, October 23–25, 2006, Grapevine, Texas*. CD-ROM.
- American Association of State Highway and Transportation Officials (AASHTO). 2004. *AASHTO LRFD Bridge Design Specifications*. 3rd ed. Washington, DC: AASHTO.
- Freyermuth, C. L. 1969. Design of Continuous Highway Bridges with Precast, Prestressed Concrete Girders. *PCI Journal*, V. 14, No. 2 (April): pp. 14–39.
- Oesterle, R. G., J. D. Glikin, and S. C. Larson. 1989. *Design of Precast Prestressed Bridge Girders Made Continuous*. NCHRP report 322I. Washington, DC: Transportation Research Board.
- American Concrete Institute (ACI) 209R-92. 1997. *Prediction of Creep, Shrinkage, and Temperature Effects in Concrete Structures*. Farmington Hills, MI: ACI.
- Peterman, R. J., and J. A. Ramirez. 1998. Restraint Moments in Bridges with Full-Span Prestressed Concrete Form Panels. *PCI Journal*, V. 43, No. 1 (January–February): pp. 54–73.
- Zia, P., H. K. Preston, N. L. Scott, and E. B. Workman. 1979. Estimating Prestress Losses. *Concrete International*, V. 1, No. 6 (June): pp. 32–38.

Notation

- b = length of joint
- E = equivalent width
- E_{deck} = modulus of elasticity of deck concrete
- $E_{precast}$ = modulus of elasticity of precast concrete
- E_{steel} = modulus of elasticity of steel
- f_c = compressive stress
- f'_c = concrete specified compressive strength
- f_{c_allow} = allowable compressive stress in concrete at transfer or under service loads
- f_{c_bottom} = compressive stress in bottom fiber
- f'_{c_CIP} = compressive strength of cast-in-place concrete
- f'_{ci} = concrete compressive strength at release
- $f'_{c_precast}$ = compressive strength of precast concrete
- f_{c_top} = compressive stress in top fiber
- f_{pu} = specified tensile strength of prestressing tendons
- f_t = tensile stress

- $f_{\tau_{allow}}$ = allowable tensile stress in concrete at transfer or under service loads
- $f_{\tau_{bottom}}$ = tensile stress in bottom fiber
- $f_{\tau_{top}}$ = tensile stress in top fiber
- h = depth of section
- l = width of joint
- l_a = loop connection total transverse length
- l_o = distance between centers of loop connection reinforcing bars
- L = length of unsupported span
- L_1 = modified span length taken equal to the lesser of the actual span or 60.0 ft
- n_d = modular ratio for cast-in-place concrete deck
- n_s = modular ratio for precast concrete section
- r = distance to the discontinuity
- s_{min} = distance between loop connection reinforcing bar and edge of joint
- s_o = loop connection reinforcing bars spacing
- W_1 = modified edge-to-edge width of bridge taken equal to 60.0 ft

About the authors



Roberto Piccinin is a technical services engineer at the Hilti Corp. in Tulsa, Okla.



Arturo E. Schultz, PhD, is a professor in the Department of Civil Engineering at the University of Minnesota.

Abstract

The precast concrete inverted-tee system was adopted by the Minnesota Department of Transportation after the 2004 FHWA/AASHTO International Scan Tour of bridge rapid construction techniques in Europe and Japan. As of 2005, two bridges were built in Minnesota adapting the Poutre-Dalle system developed in France. One of the two bridges, the Center City Bridge (MN bridge 13004), has been monitored for transverse load distribution and continuity over the pier since the deck was cast in September 2005. In addition, a two-span specimen was constructed to investigate different parameters, such as flange thickness, bursting reinforcement, horizontal shear reinforcement, and flange surface treatment. One of the four precast concrete sec-

tions of the laboratory specimen was identical to those used for MN bridge 13004. Part of the investigation was conducted to optimize section design through a parametric study. In addition, preliminary linear elastic finite element analyses were conducted to simulate the behavior of the system. The finite element models were calibrated using results obtained from static tests of MN bridge 13004 and the laboratory specimen. This paper presents a series of considerations obtained from a preliminary parametric study on different span lengths and bridge configurations. It also discusses some matters that had to be resolved to obtain acceptable agreement between experimental results and analytical approach. For all of the cases investigated, the service stresses were found to control the design.

Keywords

Bridge, cracking, FEM, finite element model, load, moment, parametric study, rapid bridge construction, slab.

Review policy

This paper was reviewed in accordance with the Precast/Prestressed Concrete Institute's peer-review process.

Reader comments

Please address any reader comments to journal@pci.org or Precast/Prestressed Concrete Institute, c/o PCI Journal, 200 W. Adams St., Suite 2100, Chicago, IL 60606. 